Structural, Conformational, and Theoretical Binding Studies of Antitumor Antibiotic Porfiromycin (*N*-Methylmitomycin C), a Covalent Binder of DNA, by X-ray, NMR, and Molecular Mechanics

S. K. Arora,*,† M. B. Cox,‡ and P. Arjunan†

Department of Crystallography, University of Pittsburgh, Pittsburgh, Pennsylvania 15260, and College of Pharmacy, University of Texas, Austin, Texas 78712. *Received October 20, 1989*

X-ray, NMR, and molecular mechanics studies on antitumor antibiotic porfiromycin ($C_{16}H_{20}N_4O_5$), a covalent binder of DNA, have been carried out to study the structure, conformation, and theoretical interactions with DNA. The crystal structure was solved by direct methods and refined to an *R* value of 0.052. The configurations at C(9), C(9a), C(1), and C(2) are *S*, *R*, *S*, and *S*, except for the orientation of the aziridine ring and (carbamoyloxy)methyl side chain. The five-membered ring attached to the aziridine ring adopts an envelope conformation. The solution conformation is similar to that observed in the solid state except for the (carbamoyloxy)methyl side chain. Monovalent and cross-linked models of the drug bound to DNA have been energetically refined by using molecular mechanics. The results indicate that, in the case of monocovalent binding, the drug clearly prefers a d(CpG) sequence rather than a d(GpC) sequence. In the case of the cross-linked model there is no clear-cut preference of d(CpG) over d(GpC), indicating that the binding preference of the drug may be kinetic rather than thermodynamic.

Introduction

Porfiromycin is an antibiotic and antitumor agent related to the mitomycins. In fact, porfiromycin is 3-*N*-methylmitomycin C as seen in Figure 1. The mitomycins were discovered in *Streptomyces caespitosus*.[1] Of the members of this family, mitomycin C is the most biologically active compound. As such, it has been the central focus of studies on this family of drugs. Clincially, porfiromycin is not used as widely as mitomycin C although the two agents show similar efficacy and toxicity. It is known that mitomycins covalently bind to DNA through alkylation. This alkylation can be either monofunctional, which is most common, or bifunctional.[2] By alkylating celluar DNA, mitomycin C inhibits DNA synthesis, interfering with cell division and cellular metabolism.[3] This property has made mitomycin C useful in the clinical chemotherapy treatment of cancer specifically in breast, gastrointestinal, and cranial tissue.[4] Mitomycin C must be reduced by enzymes or chemical reducing agents to become an active alkylating agent.[2]

The binding sites on mitomycin C have been identified[5] to be C(1) and C(10). There is direct evidence that the binding site of mitomycin C in both the monofunctional and bifunctional adducts is at the N(2) of guanine residues. This has recently been reported by Tomasz et al.[6-8] using Fourier transform infrared spectroscopy, circular dichroism, and ^{1}H NMR. Their results further indicated that the two guanine residues involved in the bifunctional adduct were not covalently bound to one another, and thus, the bifunctional adduct was an interstrand cross-link.

As the active adduct, the bifunctional alkylation product is, therefore, of structural interest. Since both binding sites require an N(2) of a guanine residue, it is most likely that the preferred sequence for the binding of mitomycin C to DNA is either d(GpC), d(CpG), or d(GpG). This is because the distance between C(1) and C(10) in mitomycin C is only long enough to span consecutive base pairs. Binding to d(GpG) would produce an intrastrand cross-link. Since only an interstrand cross-link adduct has been isolated and identified,[8] d(GpG) is not likely to be a potential binding site. Rather, d(GpC) and d(CpG) are the probable binding sites.

A recent study by Teng et al.[9] has indicated that d(CpG) is the more preferred sequence for mitomycin C binding than d(GpC). Cross-linking was not observed in any DNA molecule which contained only d(GpC) sequences without any d(CpG) sequences. It was determined that binding was increased if the multiple d(CpG) sequences were consecutive rather than dispersed in an isolated fashion throughout the DNA. Their molecular modeling studies indicated that energetically there is hardly any difference between the bifunctional adduct of mitomycin C with d(GpC) or d(CpG) sequences.

These results were rationalized by the proposal that preferred binding at d(CpG) sites as opposed to d(GpC) sites is a kinetic phenomenon rather than thermodynamic and therefore cannot be predicted by static molecular mechanics modeling.[9]

We have carried out structural and conformational studies on another drug in the mitomycin family, porfiromycin, using X-ray, NMR, and molecular modeling with the aim of comparing the conformation of porfiromycin with other mitomycins.[11-14] Porfiromycin is biologically less active than mitomycin C, and it was hoped that a structural comparison of the two compounds might provide useful information regarding structure and activity relationships within the mitomycin family of drugs. In addition, molecular mechanics modeling studies of porfiromycin and DNA adducts were carried out for comparison with recent analogous studies which had been performed on mitomycin C.[9,10,15] These were designed to contribute

† University of Pittsburgh.
‡ Present address: Vista Chemical Co., Austin, TX 78720.

(1) Hata, T.; Sano, Y.; Sugawara, R.; Kanamori, K.; Shima, T.; Hoshi, T. *J. Antibiot.* **1956**, Ser. A 9, 141.
(2) Iyer, V.; Szybalski, W. *Science (Washington, D.C.)* **1964**, *145*, 55.
(3) Goldberg, I. H.; Freeman, P. A. *Annu. Rev. Biochem.* **1971**, *40*, 775.
(4) Crooke, S. T.; Bradner, W. T. *Cancer Treat. Rep.* **1976**, *3*, 121.
(5) Moore, H. W. *Science (Washington, D.C.)* **1977**, *197*, 527.
(6) Tomasz, M.; Lipman, R. *J. Am. Chem. Soc.* **1986**, *25*, 4337.
(7) Tomasz, M.; Lipman, R.; Chowdary, D.; Pawlak, J.; Verdine, G. L.; Nakanishi, K. *Science (Washington, D.C.)* **1987**, *235*, 1204.
(8) Tomasz, M.; Chawla, A. K.; Lipman, R. *Biochemistry* **1988**, *27*, 3182.
(9) Teng, S. P.; Woodson, S. A.; Crothers, D. M. *Biochemistry* **1989**, *28*, 3901.
(10) Rao, S. N.; Singh, U. C.; Kollman, P. A. *J. Am. Chem. Soc.* **1986**, *108*, 2058.
(11) Arora, S. K. *Life Sci.* **1979**, *24*, 1519.
(12) Tulinsky, A.; Van Den Hendre, J. H. *J. Am. Chem. Soc.* **1967**, *89*, 2905.
(13) Yahashi, R.; Matsubara, I. *J. Antibiot.* **1976**, *29*, 104.
(14) Ogawa, K.; Nomura, A.; Fujiwara, T.; Tomita, K. *Bull. Chem. Soc. Jpn.* **1979**, *52*, 2334.

0022-2623/90/1833-3000$02.50/0

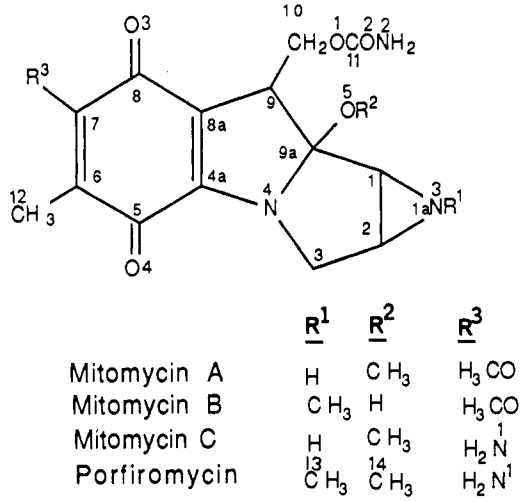

	R^1	R^2	R^3
Mitomycin A	H	CH_3	H_3CO
Mitomycin B	CH_3	H	H_3CO
Mitomycin C	H	CH_3	H_2N
Porfiromycin	$^{13}CH_3$	$^{14}CH_3$	H_2N

Figure 1. Chemical structures of mitomycins.

information to both the questions concerning the difference in activities between porfiromycin and mitomycin C and the questions regarding the binding preference of d(CpG) over d(GpC) sequences for this class of compounds.

Methods

X-ray. Porfiromycin was kindly provided by Dr. John Duros of the National Cancer Institute. Needle-shaped crystals were grown from aqueous ethanol by slow evaporation. The crystals belong to the monoclinic space group $P2_1$ with cell dimensions of a = 10.047 (4(Å, b = 8.274 (3) Å, c = 10.794 (4) Å, β = 113.32 (3)°, = 2, D_2 = 1.43 g cm^{-3}, F_w = 348.36, and V = 824.04 A^3. A crystal with dimensions of 0.2 × 0.3 × 0.3 mm was used for data collection. Intensities of 4187 reflections N±h,±k,l), 4.0 < 2θ < 53.0°, were measured using Mo Kα (λ = 0.71069 Å) radiation on a Nicolet P3 diffractometer equipped with a graphite monochromator and a Nicolet LT-1 inert gas (N_2) low-temperature delivery system (-110 °C), an Omega scan technique, variable scan rate (2.0–6.0°), a scan range of 2.0°, and a scan to background ratio of 1.0. A total of 1807 independent reflections with $I > 2.5\sigma(I)$ were considered observed. Intensities were corrected for Lorentz and polarization effects, but no absorption correction was applied.

The structure was solved by the direct methods program SHELEX86 (14) with E's > 1.2. The first E map revealed all of the 25 non-hydrogen atoms. The initial R factor with all the non-hydrogen atoms included was 0.29. The structure was first refined isotropically and the anisotropically to an R factor of 0.072. At this stage, calculated hydrogen positions were included. Further refinement using anisotropic thermal parameters for non-hydrogen atoms and isotropic thermal parameters for hydrogen atoms reduced the R factor to a final value of 0.052. The refinement was based on F_o, the quantity minimized being $\sum w(F_o - F_c)^2$ where $w = 1/\sigma(F_o)^2$. The final coordinates with standard deviations are given in Table I. These coordinates produce the stereochemistry shown to be the absolute stereochemistry of the crystal structure of a heavy atom derivative of mitomycin C.[16]

NMR. The ^{1}H spectrum was obtained on a 5.0 mM solution of porfiromycin in CDC_3 at 500.1 MHz on a GN-500 NMR spectrometer equipped with a variable-temperature thermocouple device. Typically, 32-32K fids were obtained in 4.1 s with a spectral window of 1002 Hz (20.0 ppm) and a pulse width of 5 s (flip angle 44°). The spectrum was obtained by means of quadrature-phase detection and computer alternative pulse phase with a recycle delay of 1.0 s. The final spectrum was weighted by use of 0.04 Hz line broadening and zero-filled to 64K, which results in a final digital resolution of 1.64 Hz.

The 2D COSY experiment was done with a modified (90°X-$t1$-60°X-Acq)n pulse sequence that emphasizes cross peaks. Typically 32–1K fids were obtained for each of 256-t1 increments with a spectral window in both dimensions of 4000 Hz, which was obtained in 0.256 s with a recycle delay of 2 s. The spectrum was sine-bell weighted in the second dimension and zero-filled and Gaussian sine-belled in the first dimension to obtain a final data point array of 512 × 512. The COSY spectrum of porfiromycin is shown in Figure 5.

Molecular Modeling. All modeling work was performed using the MACROMODEL version 2.0 software package developed by Dr. Clark Still of Columbia University.[17] The structures of porfiromycin and mitomycin C[11] obtained from crystallographic data were minimized by using the AMBER force field[18] and a block-diagonal Newton Raphson minimization procedure. Minimizations were carried out to a root mean square (RMS) first derivative of 0.01 Kj/A for both drug molecule models.

For the purpose of building porfiromycin–DNA adduct models, two models of the drug were constructed from the crystal structure to represent the forms (mitosenes) and drug adopts after binding to DNA both monofunctionally and bifunctionally. This was done by using double bond parameters for C(9)–C(9a) bond and planar indole nitrogen parameters for N(4). This procedure is similar to the one used in a previous modeling study performed on mitomycin C–DNA adducts by Rao et al.[10] The structures of these models are shown in Figure 6. Note that these models are not meant to represent stable intermediates of the drug which may form before binding to DNA. Rather, these are the forms of the drug hypothesized to

Table I. Coordinates for Non-Hydrogen Atoms (×10^3)

atom	x	y	z
O(1)	3471 (3)	-885 (5)	108 (2)
O(2)	3671 (3)	1472 (5)	-819 (3)
O(3)	-336 (3)	1132 (6)	818 (3)
O(4)	2520 (3)	-586 (5)	5953 (2)
O(5)	3320 (3)	-3923 (5)	2399 (3)
N(1)	-972 (3)	2654 (6)	2638 (3)
N(2)	5081 (4)	-659 (7)	-795 (4)
N(3)	5376 (3)	-214 (6)	3385 (3)
N(4)	3347 (3)	-1810 (5)	3920 (3)
C(1)	4981 (4)	-1844 (6)	2868 (4)
C(2)	5780 (4)	-1563 (6)	4325 (4)
C(3)	4793 (4)	-1783 (7)	5053 (4)
C(4a)	2284 (4)	-726 (6)	3702 (3)
C(5)	1902 (4)	-39 (6)	4805 (3)
C(6)	817 (4)	1184 (6)	4436 (3)
C(7)	78 (4)	1562 (6)	3097 (4)
C(8)	381 (4)	736 (6)	1984 (4)
C(8a)	1522 (4)	-397 (6)	2388 (3)
C(9)	2188 (4)	-1265 (6)	1540 (3)
C(9a)	3439 (4)	-2231 (6)	2625 (3)
C(10)	2658 (4)	-42 (7)	749 (4)
C(11)	4062 (4)	103 (6)	-533 (4)
C(12)	482 (4)	1955 (7)	5522 (4)
C(13)	2051 (4)	-4661 (7)	2419 (4)
C(14)	6559 (4)	468 (7)	3087 (4)

(15) Remers, W. A.; Rao, S. N.; Wunz, T. P.; Kollman, P. A. *J. Med. Chem.* **1988**, *31*, 1612.
(16) Shirahata, K.; Hirayama, N. *J. Am. Chem. Soc.* **1983**, *105*, 7199.
(17) Still, W. C.; Mohmadi, F.; Richards, N. G. J.; Guida, W. C.; Lipton, M.; Liskamp, R.; Chang, G.; Hendricckson, T.; DeGunst, F.; Hasel, W. MACROMODEL V2.5, Department of Chemistry, Columbia University, New York, NY 10027.

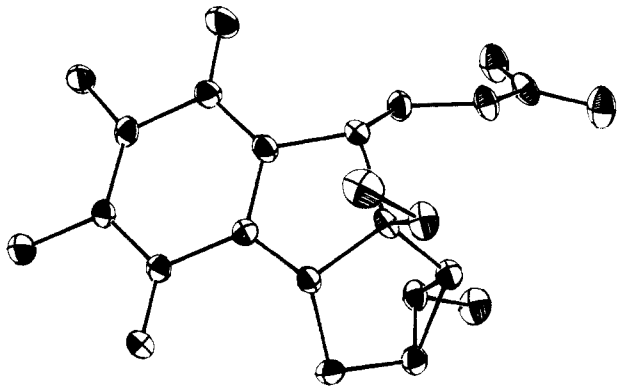

Figure 2. Thermal ellipsoid plot of porfiromycin.

be bound to the DNA and which would not necessarily be stable when separated from the DNA. These two models were minimized by using a block-diagonal Newton Raphson minimization procedure and the MACROMODEL AMBER force field of Weiner et al.[18] with all additional parameters and charges supplied by the Rao et al.[10] The addition of these supplemental parameters involved editing the MACROMODEL AMBER force field file. Special substructure modules containing the parameters for the two binding forms of porfiromycin were created by using the same format as the other substructure files found in MACROMODEL force field files. A united atom force field was used with the charges from the all atom field which were appropriate for united atom models. The MACROMODEL version of AMBER reproduced the charges of the stand alone AMBER field. A distance-dependent dielectric constant was used in all calculations. The two models were minimized to a RMS first derivative of 0.01 Kj/A.

Porfiromycin–DNA adduct models were created by docking the preminimized monofunctional and bifunctional binding form models into a model of the decamer $d(GCGCGCGCGC)_2$, hereafter referred to as GC10, visually using an Evans and Sutherland 390 graphics system. The preminimized GC10 model was generated from the standard B DNA coordinates provided in MACROMODEL. The conformation of the (carbamoyloxy)methyl chain at C(10) was slightly altered in the monofunctional models by manually rotating about the dihedral angles C(8a)–C(9)–C(10)–O(1), C(9)–C(10)–O(1)–C(11), and C(10)–O(1)–C(11)–N(2). This was done to limit unfavorable steric contacts with the DNA. This is a reasonable approximation as the chain is relatively free-rotating and flexible.

An attempt was made to reproduce the orientation depicted in the most recent mitomycin C and GC10 modeling study,[15] but this proved impossible. This is most probably due to the fact that the drug model used in this study was based on the crystal structure and therefore is slightly puckered, while the drug model used in the mitomycin C study was not derived from crystallographic studies and was planar. Translational and rotational simplex searches helped to eliminate unfavorable steric contacts. The drug models were then covalently bound to the N(2) of the guanine residues in the minor groove of the decamer. Four models were created with porfiromycin bound both monofunctionally at C(1) and bifunctionally at C(1) and C(10) to both d(CpG) and d(GpC) sequences. A schematic illustration of these models is shown in Figure 7. All four adduct models as well as the decamer itself were minimized using the modified AMBER force field described above for the binding form models and a conjugate gradient minimization method using the Perry self-correcting first derivative method with restarts. Minimizations were carried out to a RMS first derivative of 0.1 Kj/A for all adduct models.

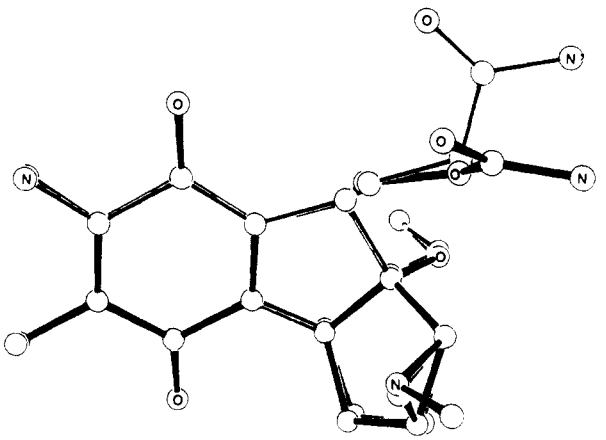

Figure 3. Comparison of the conformations of porfiromycin (thick bonds) and mitomycin C (thin bonds).

Table II. Torsion Angles (in Degrees) in the (Carbamoyloxy)methyl Side Chain from Several Mitomycin Crystal Structures

compound	θ^a	ϕ	ψ	ref
Br-Mitomycin A	−179.5	−166.2	−1.8	12
Br-Mitomycin B	−298.5	−160.1	−344.8	13
Br-Mitomycin C	−180.5	−280.7	−353.9	14
Mitomycin C	−182.4	−244.0	−2.3	14
Mitomycin C	−179.5	121.7	−0.4	11
Porfiromycin	171.8	−174.4	−16.9	

[a] θ = C(8a)C(9)–C(10)–O(1). [b] ϕ = C(9)–C(10)–O(1)–C(11). [c] ψ = C(10)–O(1)–C(11)–O(2).

Results and Discussion

Figure 2 shows the stereochemistry of the molecule. The bond lengths and angles in the porfiromycin molecule agree with those observed in mitomycin structures studied previously.[11-14] The geometry of the benzoquinone portion of the molecule, with C(7)–C(8) = 1.513 Å and C(4a)–C(8a) = 1.346 Å, is similar to that of the resonance structures given by Kulpe.[19,20] The benzoquinone ring is slightly deviated from planarity. N(4) behaves as an amide nitrogen due to its participation in the conjugated benzoquinoid system and is deviated 0.293 Å from a plane calculated through C(3), C(4a), and C(9a). The bond angles around N(4) are more tetragonal in character than trigonal. The five-membered ring attached to the benzoquinone ring is approximately planar, while the other five-membered ring adopts an envelope conformation similar to that observed in the other mitomycin structures. The configurations at C(9), C(9a), C(1), and C(2) are *S*, *R*, *S*, and *S*, respectively. The plane of the aziridine ring makes a 112.5° angle with the adjacent indole ring. This differs by approximately 31° from that observed in mitomycin C.[11] This difference is observable in Figure 3 and is due to the presence of the methyl group at N(3) of porfiromycin. The trans arrangement of the (carbamoyloxy)methyl and the methoxyl groups at C(9) and C(9a), respectively, is similar to that observed in mitomycins A and C and most probably prevents short intramolecular contacts between these groups. The conformation of the (carbamoyloxy)methyl side chain in the solid state is different in porfiromycin and mitomycin C. The major

(18) Weiner, S. J.; Kollman, P.; Case, D.; Singh, U. C.; Ghio, C.; Alogna, G.; Weiner, P. *J. Am. Chem. Soc.* **1984**, *106*, 765.

(19) Kulpe, S. *Acta Crystallogr.* **1969**, *B25*, 1411.

(20) Kulpe, S. *J. Prakt. Chem.* **1971**, *312*, 909.

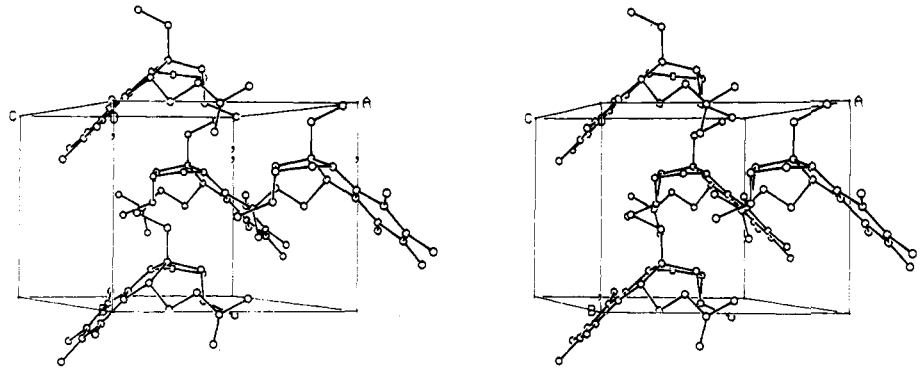

Figure 4. Packing of the porfiromycin molecules in the unit cell.

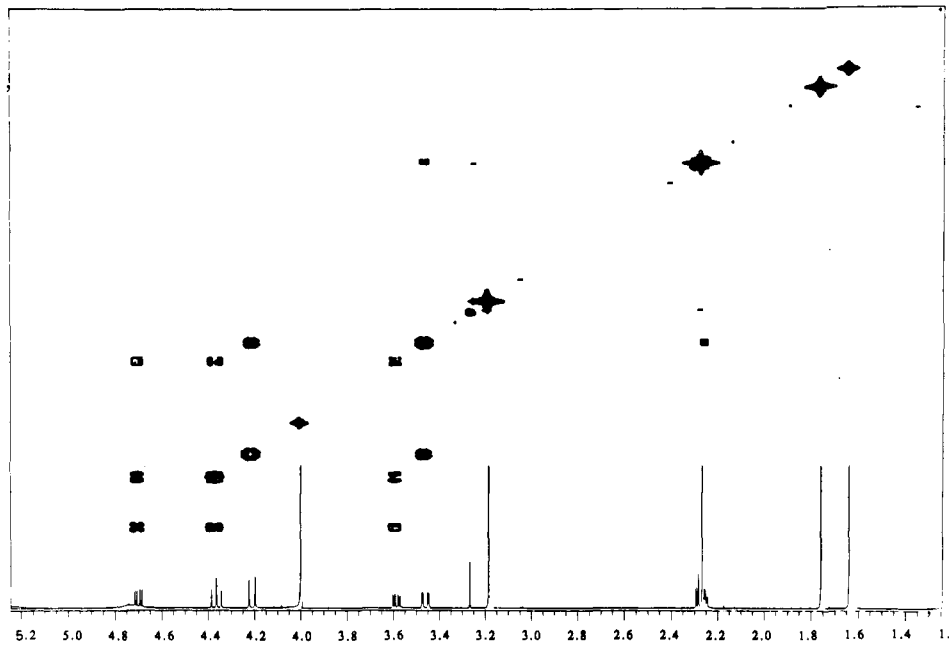

Figure 5. 2-D COSY spectrum (500 MHz) of porfiromycin in $CDCl_3$.

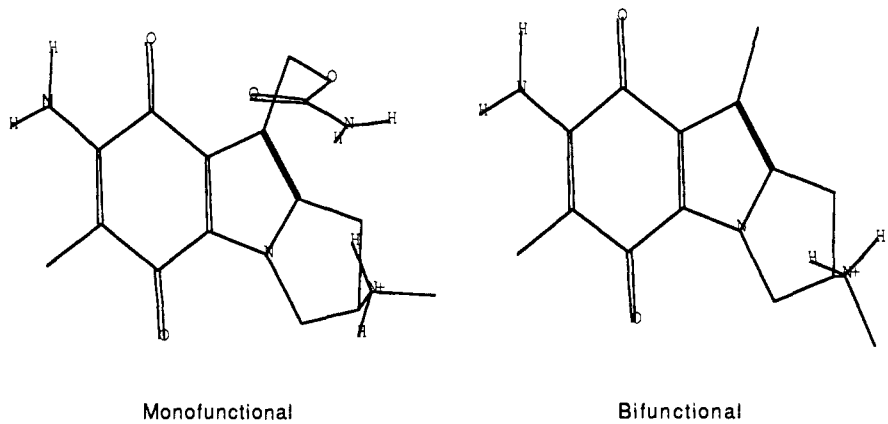

Figure 6. Monofunctional and bifunctional binding forms of porfiromycin.

difference is in the dihedral angle C(9)–C(10)–O(1)–C(11), which has a value of −174.4° in porfiromycin and 121.7° in mitomycin C. The porfiromycin angle is closer to the angle seen in mitomycin B than that seen in mitomycin C. This could be due to the presence of the methyl groups at C(9a) and N(1). Figure 3a also compares this side chain with that of mitomycin C. Table II gives a comparison of the torsion angles in the (carbamoyloxy)methyl chain in different mitomycins. The differences may be due to the different packing forces in each crystal, indicating the flexibility of this chain. Figure 4 shows the packing of the molecules in the unit cell. There are two intermolecular hydrogen bonds: (1) N(1)–H···O(4) ($-x$, $^1/_2 + y$, $1 - z$) with a distance of 2.953 Å and (2) N(2)–H···O(2) ($1 - x$, $-^1/_2y$, $-z$) with a distance of 2.918 Å. The only intramolecular hydrogen bond involves N(1) and O(3) with a distance of 2.611 Å.

High-resolution NMR studies were conducted to assign the proton resonances in porfiromycin, as well as to compare the conformation of this antibiotic in the solid state and in solution. A 500-MHz ^1H spectrum was obtained as detailed in the Methods section. All the protons have been assigned except those of the amine. Figure 5 shows the 2D COSY spectrum of porfiromycin. The cross peaks

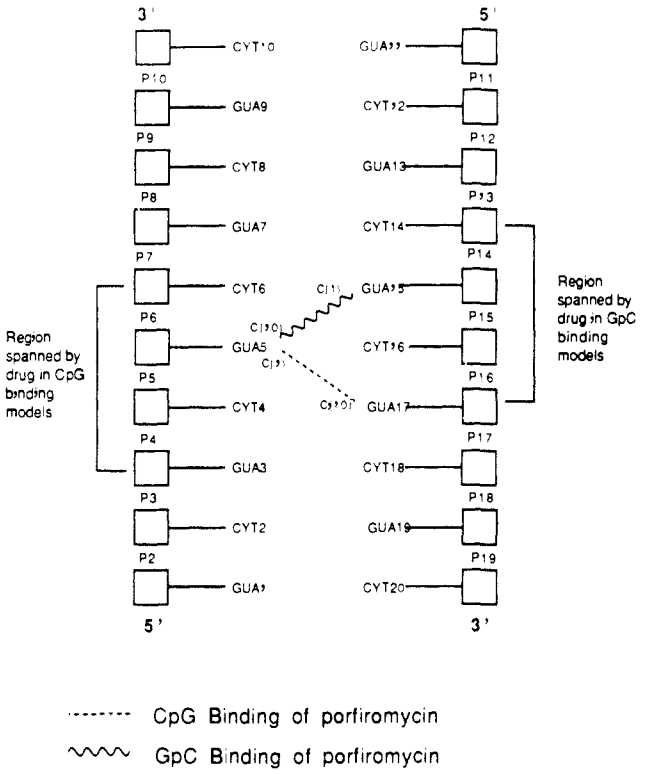

Figure 7. Schematic illustration of porfiromycin and d-(GCGCGCGCGC)$_2$ adduct models.

Table III. Chemical Shifts, Coupling Constants, Dihedral Angles (in Degrees) for Porfiromycin

assignment	chemical shift	coupling constant, Hz	θ_{NMR}[a]	$\theta_{X\text{-}ray}$[b]	θ_{min}[c]
HC1	4.20	$J_{1,2}$ = 12.95	175	0.8	7.5
HC2	3.45	$J_{1,2}$ = 12.95	175	0.8	7.5
		$J_{2,3'}$ = 2.13	80 (95)	83.3 (−39.1)	80.2 (−45.8)
H′C3	2.25	$J_{2,3'}$ = 2.12	80 (95)	83.3 (−39.1)	80.2 (−45.8)
		$J_{3',3''}$ = 4.68			
H″C3	2.28	$J_{3',3''}$ = 4.68			
HC12	1.75				
HC9	4.36	$J_{9,10}$ = 10.76	10 (152)	52.5 (172.9)	55.0 (176.9)
H′C10	3.59	$J_{9,10'}$ = 10.93	5 (153)		
		$J_{10',10''}$ = 4.43			
H″C10	4.70	$J_{9,10''}$ = 10.61	14 (151)		
		$J_{10',10''}$ = 4.43			
HC13	3.18				
HC14	2.26				
H_2O	1.64				

[a] For θ_{NMR}, other values possible for this angle are given in parentheses. [b] For $\theta_{X\text{-}ray}$, since H′C3/H″C3 and H′C10/H″10 of the NMR study cannot be assigned specifically to H(1)C(3)/H(2)C(3) and H(1)-C(10)/H(2)C(10) of the crystal study, the dihedral angles of both hydrogens on C(3) and C(10) are given in parentheses. [c] For θ_{min}, same as for $\theta_{X\text{-}ray}$ in footnote *b*.

from the protons having dihedral angles between 65 and 100°, and thus having small J(H–H), are not clearly observed. Table III gives the chemical shifts, the coupling constants, and the calculated dihedral angles obtained from the NMR spectrum. The dihedral angles obtained from X-ray and from NMR vary in the (carbamoyloxy)-methyl side chain. This indicates the flexibility of this side chain.

Molecular mechanics calculations were carried out on both porfiromycin and mitomycin C. The initial and used were those from the crystallographic studies. The energy difference between the X-ray and the energy-minimized structure of porfiromycin was 33.4 kcal. This large difference in energy is most probably due to the difference in bond lengths, angles, and torsion angles. Table IV compares the torsion angles from the X-ray and the energy-minimized structures for porfirmoycin and mitomycin C. These dihedral angles agree reasonably well. One interesting difference is that, although the angle C(9)–C-(10)–O(1)–C(11) in porfiromycin and mitomycin C differs in the solid state by 63.9°, in the energy-minimized structures this difference is only 3.6°. Thus, in the energy-minimized structure, the mitomycin C molecule adopts a conformation very similar to that of porfiromycin. The other major difference between the crystal and energy-minimized structures of porfiromycin involves the torsion angle C(3)–C(2)–N(3)–C(1) with the values being −100.5 and −130.8 for the crystal and minimized structures, respectively.

Table IV. Selected Torsion Angles[a]

atoms	porfiromycin		mitomycin C	
	X-ray	MM2	X-ray	MM2
C(9)–C(10)–O(1)–C(11)	−174.4	−172.4	121.7	−168.8
C(10)–O(1)–C(11)–O(2)	−16.9	−1.4	−0.4	−1.7
C(10)–O(1)–C(11)–N(2)	163.8	178.2	179.8	178
N(4)–C(9a)–O(5)–C(13)	56.4	40.0	50.0	41.0
C(1)–C(9a)–O(5)–C(13)	167.4	150.8	159.2	150.7
C(9)–C(9a)–O(5)–C(13)	−61.2	−78.3	−68.3	−77.3
C(9a)–N(4)–C(3)–C(2)	21.3	21.3	26.1	24
N(4)–C(3)–C(2)–C(1)	−12.9	−3.5	−13.0	−4.2
C(3)–C(2)–C(1)–C(9a)	0.8	−13.2	−3.4	−14.3
C(2)–C(1)–C(9a)–N(4)	11.8	22.9	18.3	25.2
C(1)–C(9a)–N(4)–C(3)	−21.2	−29.7	−28.1	−33.2
N(4)–C(3)–C(2)–N(3)	51.7	60.2	50.6	59.8
C(3)–C(2)–N(3)–C(1)	−100.5	−130.8	−100.6	−104
C(3)–C(2)–N(3)–C(14)	155.6	150.4		
C(2)–N(3)–C(1)–C(9a)	98.7	90.8	98.1	89.5
C(9a)–C(1)–N(3)–C(14)	−154.6	−161.0		
N(4)–C(9a)–C(1)–N(3)	−51.8	−39.6	−46.5	−37.1
C(8a)–C(9)–C(10)–O(1)	171.8	176.5	−179.5	174.9
C(9a)–C(9)–C(10)–O(1)	57.5	62.9	65.2	61.6

[a] The angles are from X-ray and energy-minimized structures of porfiromycin and mitomycin C.

Table V. Energies[a] for Minimized DNA and Porfiromycin Complexes (kcal)

complex	CpG MONO	CpG BI	GpC MONO	GpC BI
total energy	−804.03	−841.70	−782.12	−831.19
drug energy	75.01	104.39	73.40	104.91
DNA energy	−877.23	−875.52	−877.94	−870.13
drug distortion	6.03	6.61	4.42	7.13
DNA distortion	24.34	26.05	23.63	31.44
interaction	−32.18	−103.23	−5.63	−104.54
net binding	−1.81	−70.57	22.42	−65.97
DNA Energy (Min)	−901.57			
Mono Energy (min)	68.98			
Bi Energy (Min)	97.78			

[a] The calculated energies are not actual free energies but molecular mechanics energies that can only be used to interpret the models qualitatively in comparison with experimental data.

Molecular mechanics studies were also performed on monofunctional and bifunctional adducts of porfiromycin bound to both d(CpG) and d(GpC) DNA sequences as described in the Methods section. Figures 8 and 9 show the energy-minimized structures of porfiromycin monofunctionally bound to d(CpG) and d(GpC) sequences, respectively. Energy data for these models is given in Table V. The d(CpG) monofunctional mode is 21.91 kcal lower in energy than the d(GpC) monofunctional model in terms of total energy and 24.23 kcal lower in terms of net binding energy. Thus, the d(CpG) sequence appears to be the energetically favored binding site for monocovalent binding.

This observation can partially be explained by examining the hydrogen-bonding patterns for these two models. The hydrogen bonds found in each model are given in Table VI. The d(CpG) model shows extensive intermo-

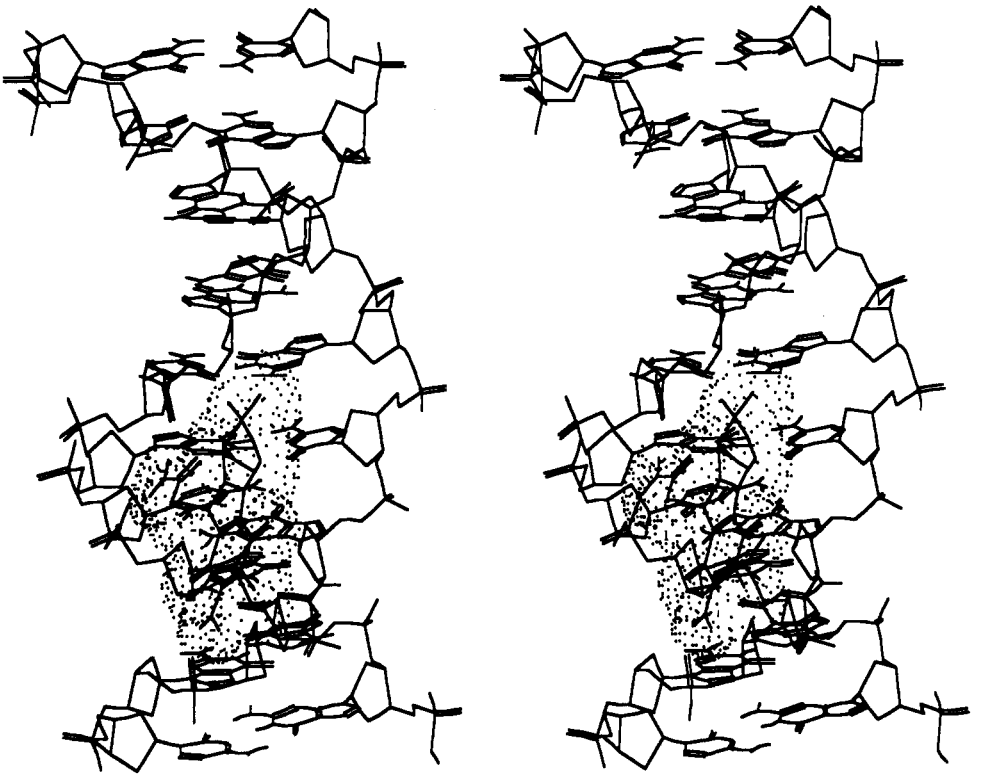

Figure 8. d(CpG) monofunctional complex of porfiromycin and $d(GCGCGCGCGC)_2$.

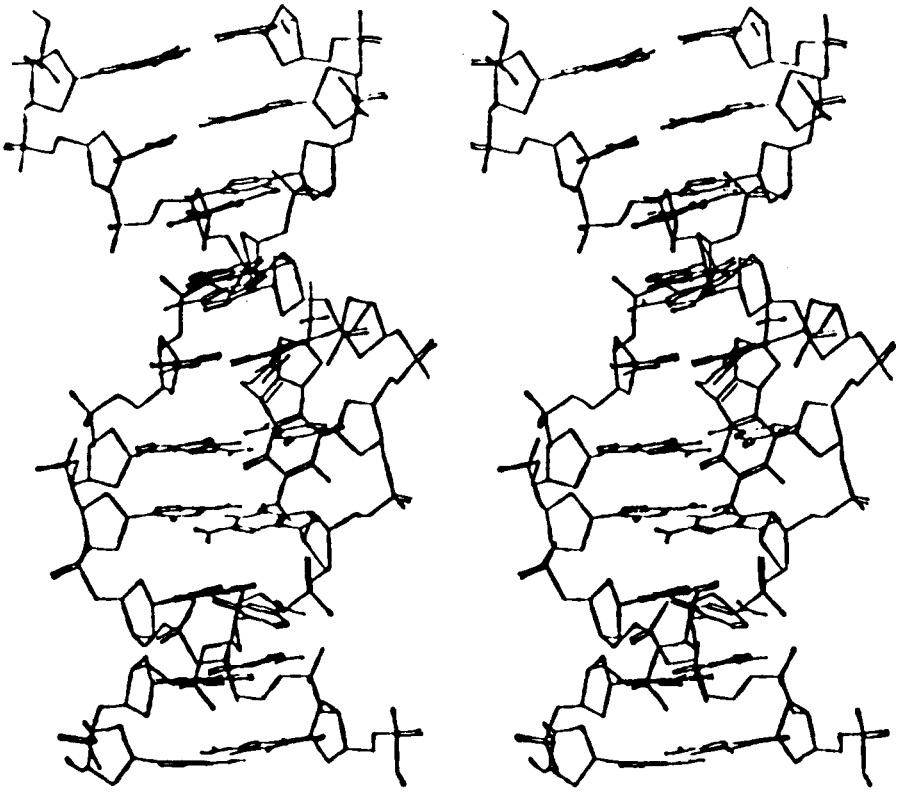

Figure 9. d(GpC) monofunctional complex of porfiromycin and $d(GCGCGCGCGC)_2$.

lecular hydrogen bonding through N(3) and N(2) of the side chain of the drug not seen in the d(GpC) model. In the d(CpG) model, N(3) lies close to CYT6 and therefore hydrogen bonds with the O(2) of this residue. In the d-(GpC) model, however, N(3) lies closest to GUA7 which has only an N2 extending into the minor groove. Since N2 is a hydrogen-bond donor, and since the N3 of GUA7, the closest hydrogen bond acceptor, is too far removed, N(3) of porfiromycin is not involved in hydrogen bonding with the DNA. The N(2) of the side chain in the d(CpG) model fits into a pocket formed by the backbone of the DNA and the smooth surface of GUA5 residue extending from its N(9) to its N(2) atoms. This allows the flexible side chain to position itself appropriately for hydrogen bonding to the backbone. However, in the d(GpC) model, the side chain is closest to CYT6 rather than to GUA5. The pocket formed by GUA5 in the d(CpG) model cannot be formed in the d(GpC) model using CYT6 because the

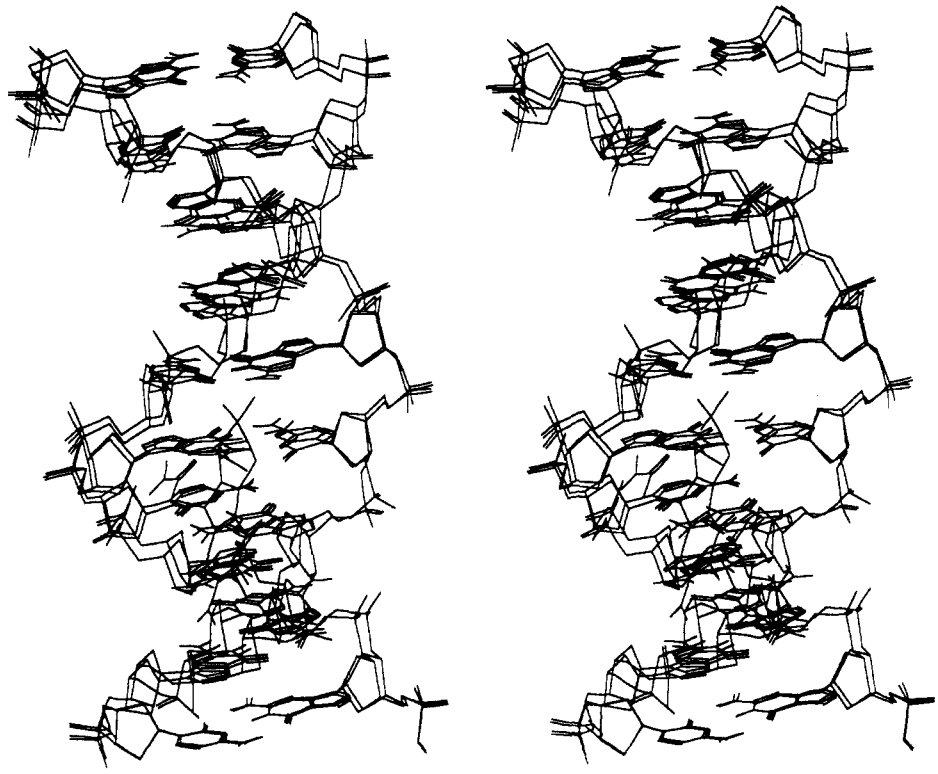

Figure 10. d(CpG) cross-linked complex of porfiromycin and $d(GCGCGCGCGC)_2$.

Table VI. Hydrogen Bonding in Porfiromycin and GC10 Complexes

complex	bond (donor–acceptor)	distance, Å	angle, deg
CpG MONO	N(1)–OP[GUA19]	2.662	154.1
	N(2)–OP[GUA7]	2.638	158.5
	N(3)–O(2)[CYT6]	2.889	138.5
CpG BI	N(1)–OP[GUA19]	2.666	138.8
	N(3)–O(1′)[CYT6]	2.769	139.5
	N(3)–O(2)[CYT6]	2.838	167.0
GpC MONO	N(1)–OP[CYT18]	2.659	157.7
	N2[GUA5]–O(3)	2.920	142.7
GpC BI	N(1)–OP[CYT18]	2.651	143.9
	N(3)–N3[GUA7]	2.880	164.6
	N(3)–O(1′)[GUA7]	2.837	150.6

O(2) of this residue extends outward into the area where the pocket should form. Due to this interference, the side chain in the d(GpC) model is sterically fored out into the minor groove rather than being tucked in close to the backbone of the DNA. The side chain cannot position itself favorably for hydrogen bonding with the backbone, and its N(2) atom is extended out of the minor groove. Thus, the fact that the d(CpG) model allows a better fit of porfiromycin which promotes hydrogen bonding may be one factor in explaining the apparent energetic preference for d(CpG) rather than for d(GpC) binding.

Analysis of the phase angle of pseudorotation P and amplitude Tm[21] of the sugar as well as the glycosidic angle χ for the residues of the DNA which span the binding site of porfiromycin was carried out (supplementary material, Table VII). In both monofunctional models, all of the glycosidic angles retain an anti conformation with slight deviation from the values observed in the minimized GC10 model. The bases adjust their positions slightly to accommodate the binding of porfiromycin. Most of the sugars remain puckered in a conformation within ±18° of the 2′-endo conformation of B DNA. Only the sugars of CYT4 and GUA17 in the d(CpG) model and CYT16 in the d(GpC) model deviate from the 2′-endo conformation. These three sugars adopt conformations in the 1′-exo region. Neither monofunctional model contains any sugars deviating toward a 3′-endo pucker, as would be seen in A DNA.

An examination the C1′ to C1′ distances (supplementary material) between bases located across the minor groove from one another of this data reveals that minor changes seem to occur in the width of the minor groove in the regions which the bound drug spans when compared with the widths seen in the GC10 model. Outside the span of the drug, the width of the minor groove remains virtually unchanged. These slight alterations indicate that, although the DNA generally remains in the B conformation upon drug binding, some slight adjustments are made in the DNA conformation to accommodate the drug. These alterations do not disrupt the hydrogen bonidng between any base pair, although in both the d(CpG) and the d(GpC) monofunctional models the [GUA3-CYT18] base pair is slightly bent from planarity. The overlapping of DNA from the d(CpG) monofunctional model with minimized GC10 by a least-squares fit gave RMS deviation of 1.3. This indicated the lack of major differences between the conformations of the two DNA molecules. Thus the DNA retains a general B DNA conformation.

The monofunctional adduct models are mainly of interest as intermediates leading to the biologically active bifunctional adducts. The conformational characteristics of the bifunctional models, however, are of primary interest. Figures 10 and 11 show the energy-minimized models of porfiromycin bound to d(CpG) and d(GpC) sequences of GC10, respectively. The energy data for these two models are included in Table V. The energy differences between the two bifunctional models are much less than those seen between the two monofunctional models. The d(CpG) model is lower in total energy than the d(GpC) model by 10.51 kcal. However, the d(CpG) model is 4.60 kcal higher than the d(GpC) model in terms of net

(21) Altona, C.; Sundaralingam, M. *J. Am. Chem. Soc.* **1971**, *94*, 8205.

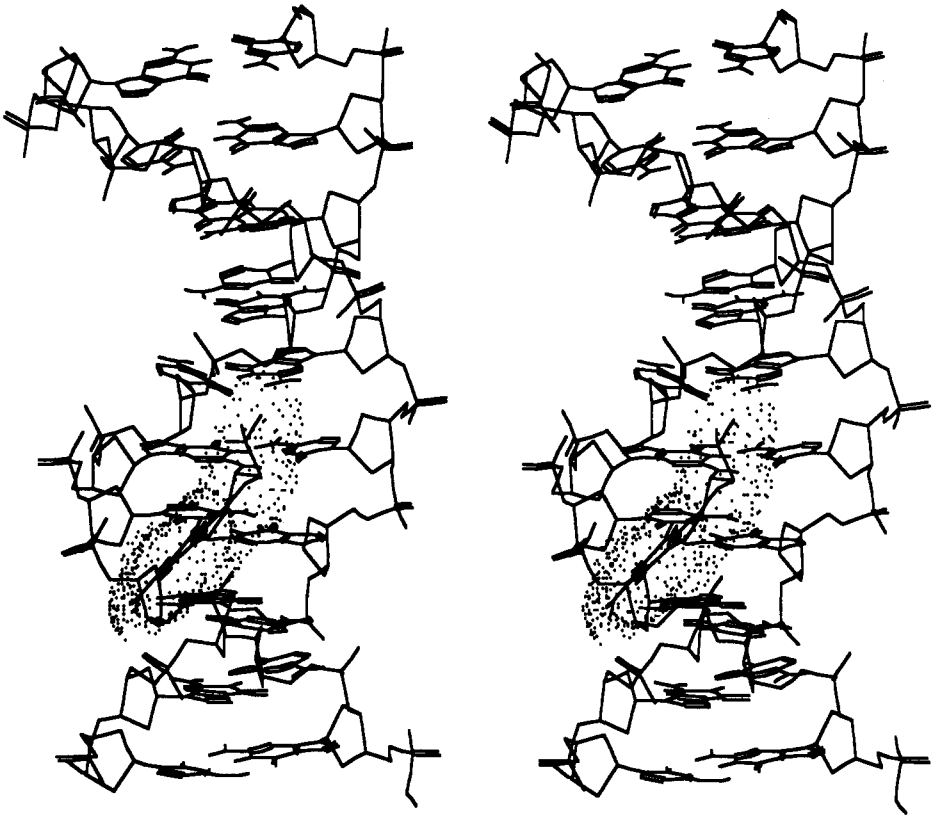

Figure 11. d(GpC) cross-linked complex of porfiromycin and $d(GCGCGCGCGC)_2$.

binding energy. Thus, as seen in the previous modeling study on mitomycin C[9] described in the introduction, the d(CpG) model does not seem to be energetically preferable to the d(GpC) model.

The structural characteristics of the two models are as similar as their energy characteristics. The hydrogen bonds found in the two bifunctional models are included in Table VI. In both models, N(1) of the drug forms hydrogen bonds to the backbone of the DNA, and N(3) forms hydrogen bonds both to the backbone and to the base of the residue immediately on the 5′ side of the binding site on the DNA strans opposite the binding site. Thus, in both models, the drug seems to fit the binding site equally well. In neither bifunctional model is any disruption between the hydrogen bonding between base pairs seen. Also, except for a very slight bending in the [GUA3·CYT18] base pair in the d(GpC) model, all of the base pairs retain planar stacking. Again, analysis of the *P*, Tm, and χ values for the residues spanning the binding region of the drug for bifunctional models was carried out (supplementary material). As in the monofunctional models, the glycosidic angles all retain an anti orientation. Unlike the monofunctional models, all of the sugars of these residues retain a conformation within ±18° of the pure 2′-endo conformation. Thus, all sugars retain a conformation similar to that observed in B DNA. Slight deviations from the B DNA conformation are seen, however, by examining the interstrand C1′–C1′ distances (supplementary material). Again, like the monofunctional models, minor changes are seen in the width of the minor groove in the region of the DNA that the drug spans. These changes are due to very small alterations in the general B DNA conformation to accommodate the presence of the drug molecule. In general, however, in both bifunctional models, the presence of the drug seems to have almost no effect on the general conformation of the DNA. The overlapping of DNA from the d(CpG) bifunctional model with minimized GC10 by a least squares fit gave a RMS deviation of 1.1° indicating that in the bifunctional models, the DNA retains a general B DNA conformation. In fact, the drug molecule seems to fit very neatly into the binding site without greatly distorting the DNA. In addition, the two bifunctional models of porfiromycin bound to GC10 indicate that the binding of the drug to d(CpG) or d(GpC) consequences yields adducts which are very similar, both energetically and conformationally.

If the d(CpG) and d(GpC) bifunctional models are to similar, how can the d(CpG) binding preference of the mitomycin family of antibiotics be explained? As discussed in the introduction, it has been suggested[9] that the binding preference of these drugs may be kinetic rather than thermodynamic. The data from this porfiromycin modeling study also indicate that this may be the case. Although the bifunctional models showed little difference, the monofunctional models showed large differences both in both energy and conformational fit of the drug in the minor groove, with the d(CpG) model being preferable in both cases. As intermediates leading to bifunctional binding, monofunctional adducts are important kinetically. If the d(CpG) monofunctional adduct is more readily formed than the d(GpC) monofunctional adduct by virtue of its lower energy, then naturally the d(CpG) bifunctional adduct will be more readily formed than the d(GpC) adduct even though there is little energy difference between the bifunctional adducts. It is merely a matter of which monofunctional intermediate is more readily available. In addition, as was mentioned in the mitomycin study,[9] it was observed that the distance between the N(2) functionalities of the two successive guanines involved in drug binding changed less for d(CpG) adducts than for d(GpC) adducts. In the d(CpG) bifunctional binding model in this porfiromycin study, the N(2) to N(2) distance is 3.54 Å compared to 3.82 Å in the minimized B DNA, a difference of 0.28 Å. For comparison, the N(2) to N(2) distance for the d(GpC) bifunctional model is 2.94 Å, compared to a minimized B DNA value of 3.79 Å, a difference of 0.85 Å. This

shrinking of the N(2) to N(2) distances may not constitute a major energy difference between the two models, but it does indicate that the d(GpC) adduct requires a larger conformational change, which might occur at a slower rate than the smaller conformational change required for d(CpG) binding. Thus, the d(CpG) bifunctional adduct may be more rapid-forming than the d(GpC) bifunctional adduct. This gives an advantage to the formation of the d(CpG) bifunctional adduct, even if it is similar in energy to the d(GpC) bifunctional adduct.

Acknowledgment. The authors thank Dr. John Duros of NCI for supplying the porfiromycin and Dr. W. C. Still of Columbia University for providing the MACROMODEL software.

Registry No. $C_{16}H_2ON_4O_5$, 801-52-5.

Supplementary Material Available: Tables of phase angles of pseudorotation, C(1')-C(1') distances, bond lengths, angles, anisotropic thermal parameters, and figures showing overlap of drug-bound and drug-free minimized DNA structures (7 pages). Ordering information is given on any current masthead page.

DNA-Directed Alkylating Agents. 2. Synthesis and Biological Activity of Platinum Complexes Linked to 9-Anilinoacridine

Brian D. Palmer,† Ho H. Lee,† Paul Johnson,† Bruce C. Baguley,† Geoffrey Wickham,‡ Laurence P. G. Wakelin,‡ W. David McFadyen,§ and William A. Denny*,†

Cancer Research Laboratory, University of Auckland School of Medicine, Private Bag, Auckland, New Zealand, Molecular Pharmacology Group, Peter MacCallum Cancer Institute, 481 Little Lonsdale Street, Melbourne, Victoria 3000, Australia, and School of Science and Mathematics Education, Institute of Education, University of Melbourne, Parkville, Victoria 3052, Australia. *Received March 6, 1990*

Two different classes of *cis*-diaminedichloroplatinum(II) complexes linked to the DNA-intercalating chromophore 9-anilinoacridine have been synthesized and evaluated as DNA-targeted antitumor agents. Two different Pt chelating ligands were investigated (based on 1,2-ethanediamine and 1,3-propanediamine), designed to deliver the Pt in an orientation likely to respectively enhance either intrastrand or interstrand cross-linking. Although both sets of ligands were somewhat unstable under neutral or basic conditions with respect to disproportionation, the corresponding Pt complexes, once prepared, appeared to be quite stable. All the Pt complexes were monitored for purity by TLC, HPLC, and FAB mass spectra, and the mode of Pt coordination was established by ^{195}Pt NMR spectroscopy. The complexes appeared to cause simultaneous platination and intercalative unwinding of plasmid DNA. In vitro studies were carried out with both wild-type and cisplatin-resistant P388 cell lines. Whereas cisplatin itself and the ethylenediamine and 1,3-propanediamine complexes used as standards were about 10-fold less active against the resistant line, the ethylenediamine-linked Pt complexes showed no differential toxicity between the two lines and the propanediamine-linked complexes showed significant differentials (up to 8-fold) in favor of the cisplatin-resistant line. However, these were no greater than those shown by the unplatinated ligands themselves. The majority of the acridine complexes were inactive in vivo against the wild-type P388 leukemia. They were very insoluble, and although a suitable formulation was found, this may have been a factor. It is also possible that these compounds bind in such a way as to direct the Pt away from the major groove.

Cisplatin (*cis*-diamminedichloroplatinum(II)) (1) is one of the very few drugs with significant clinical activity against a range of solid tumors[1] and is therefore widely used despite its severe side effects[2] and steep dose–response curve.[3] The primary mechanism of cytotoxicity of cisplatin and analogues is by initial cross-linking of cellular DNA (primarily through the N7 of guanine,[4] although bonding to both N1 and N3 of purines has also been reported[5]). However, the relative importance of the more common intrastrand cross-linking compared with the much less common (<1% of total platination)[6] but potentially more lethal interstrand cross-links has yet to be decided. The actual bonding to DNA occurs via the aquo species, with relatively slow kinetics compared to that of the organic alkylators, especially for the second step to form the cross-link, which can take some hours.[7] The development of cellular resistance to cisplatin in mammalian cells is common, via three main mechanisms:[8] (1) increased efficiency of repair of platinum–DNA lesions,[9,10] (2) increased inactivation of drug by elevated levels of cellular low-molecular weight thiols, particularly glutathione,[11] and (3) decreased cellular uptake of drug.[12,13]

Many analogues of cisplatin have been prepared, where the labile chloro ligands have been replaced by other leaving groups (e.g. carboplatin (2)) and/or the stable

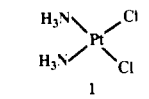

1

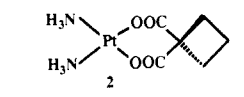

2

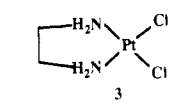

3

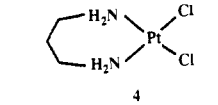

4

amine ligands have been extended by a series of either cyclic or acyclic alkyldiamines [e.g. dichloro(ethylenedi-

† University of Auckland School of Medicine.
‡ Peter MacCallum Cancer Institute.
§ University of Melbourne.

(1) Loehrer, P. J.; Einhorn, L. H. *Ann. Internal Med.* **1984**, *100*, 704.
(2) Dabrowiak, J. C.; Bradner, W. T. In *Progress in Medicinal Chemistry*; Ellis, G. P., West, G. B., Eds.; Elsevier Science Publishers: New York, 1987; Vol. 24, pp 129–158.
(3) Abrams, J. *Eur. J. Cancer Clin. Oncol.* **1986**, *22*, 9.
(4) Sherman, S. E.; Gibson, D.; Wang, A. H-J.; Lippard, S. J. *Science* **1985**, *230*, 412.
(5) Raudaschl-Sieber, G.; Schollhorn, H.; Thewalt, U.; Lippert, B. *J. Am. Chem. Soc.* **1985**, *107*, 3591.
(6) Eastman, A. *Pharmacol. Ther.* **1987**, *34*, 155.
(7) Schaller, W.; Reisner, H.; Holler, E. *Biochemistry* **1987**, *26*, 943.
(8) de Graeff, A.; Slebos, R. J. C.; Rodenhuis, S. *Cancer Chemother. Pharmacol.* **1988**, *24*, 325.
(9) Eastman, A.; Schulte, N. *Biochemistry* **1988**, *27*, 4730.
(10) Masuda, H.; Ozols, R. F.; Lai, G-M.; Fojo, A.; Rothenburg, M.; Hamilton, T. C. *Cancer Res.* **1988**, *48*, 5713.
(11) Hromas, R. A.; Andrews, P. A.; Murphy, M. P.; Burns, C. P. *Cancer Lett.* **1987**, *34*, 9.

0022-2623/90/1833-3008$02.50/0